Submitted to The Astrophysical Journal
Preprint typeset using LaTeX style emulateapj v. 11/12/01

FUTURE EVOLUTION OF COSMIC STRUCTURE IN AN ACCELERATING UNIVERSE

Michael T. Busha, Fred C. Adams[1], Risa H. Wechsler, and August E. Evrard[1]
Michigan Center for Theoretical Physics
Physics Department, University of Michigan, Ann Arbor, MI 48109
mbusha, fca, wechsler, evrard@umich.edu
Submitted to the ApJ 2003 April 23

ABSTRACT

Current cosmological data indicate that our universe contains a substantial component of dark vacuum energy that is driving the cosmos to accelerate. We examine the immediate and longer term consequences of this dark energy (assumed here to have a constant density). Using analytic calculations and supporting numerical simulations, we present criteria for test bodies to remain bound to existing structures. We show that collapsed halos become spatially isolated and dynamically relax to a particular density profile with logarithmic slope steeper than -3 at radii beyond r_{200}. The asymptotic form of the space-time metric is then specified. We develop this scenario further by determining the effects of the accelerating expansion on the background radiation fields and individual particles. In an appendix, we generalize these results to include quintessence.

Subject headings: cosmology:theory — large-scale structure of universe — dark matter — dark energy

1. INTRODUCTION

The past several years have witnessed an impressive solidification of our estimates for the basic cosmological parameters. Measurements of the cosmic microwave background radiation indicate that the cosmos is spatially flat (e.g., Hanany et al. 2000). Observations of Type Ia supernovae suggest that the universe is accelerating (Riess et al. 1998; Perlmutter et al. 1998; Garnavich et al. 1998). These data, in conjunction with additional observations of the large-scale galaxy distribution (e.g., Peacock et al. 2001) and the Hubble constant (Freedman et al. 2001), argue for a specific cosmological model with matter density $\Omega_{\rm m,0} \simeq 0.3$, dark vacuum energy density $\Omega_{\rm v,0} \simeq 0.7$, curvature constant $k = 0$, and Hubble constant $H_0 \simeq 70$ km s^{-1} Mpc^{-1}. This cosmological model has recently received impressive validation by results from the WMAP satellite (Bennett et al. 2003). In combination with data on the Hubble constant, large-scale structure, and they Lyman-α forest, WMAP constrains the values of these parameters to a few percent (Spergel et al. 2003).

In this newly consolidated cosmological model, the most unexpected property is the large (apparent) energy density in the form of dark vacuum energy. The substantial value of $\Omega_{\rm v,0} = 0.7$ produces a correspondingly large effect on past cosmological evolution. In particular, the age of the universe is somewhat longer than in a flat cosmology with no vacuum energy and more consistent with other age indicators (e.g., Carroll, Press, & Turner 1992). But, by far, the most striking consequence of this vacuum energy lies in our cosmological future.

If the universe is already starting to accelerate, as indicated by the observationally implied value $\Omega_{\rm v,0} = 0.7$, then structure formation is virtually finished. In the relatively near future, the universe will approach a state of exponential expansion and growing cosmological perturbations will freeze out on all scales. Existing structures will grow isolated. In the face of such desolation, we would like to know more quantitatively the conditions required for the formation (collapse) of future cosmological structures and the conditions required for small bodies to remain bound to existing structures. We would also like to know the asymptotic form of the existing cosmological structures, in particular the dark matter halos. By answering these questions, we can determine how much structure formation remains to occur in the future of our universe.

Given the relatively well constrained parameters of our universe, the future evolution of cosmological structure can now be predicted with some confidence. Indeed, several recent papers have begun to explore this issue. Possible future effects of vacuum energy density were outlined in a recent review of our cosmic future (Adams & Laughlin 1997, hereafter AL97). As the universe accelerates, currently visible galaxies are redshifted out of view and will become inaccessible to future astronomers (Loeb 2002). Simulations of future structure formation have been done for the case of a cosmological constant with a focus on our local portion of the universe (Nagamine & Loeb 2002). Similar issues have been explored semi-analytically, including basic effects of quintessence (Chieuh & He 2002; Gudmundsson & Björnsson 2002). A comprehensive list of papers related to the future evolution of the universe is compiled in Cirkovic (2003).

In this paper, we consider the future evolution of structure formation with a constant density of dark vacuum energy. We extend previous work by deriving analytic estimates for the conditions required for the collapse of structures, and by analyzing the results from a suite of numerical simulations of future structure formation. The future evolution of cosmic structure can be viewed in two related ways. The traditional approach considers whether or not a given region of the universe with overdensity $\delta_0 \equiv (\rho - \langle\rho\rangle)/\langle\rho\rangle$ will collapse. Given the strong suppression of future structure formation, however, relatively little will happen in terms of new formation. A related question is to ask whether or not test bodies will remain bound to

[1] Astronomy Department, University of Michigan, Ann Arbor, MI 48109

existing structures. This issue operates on a wide range of spatial and mass scales: Will the local group remain bound to the Virgo cluster? Will a satellite dwarf galaxy remain bound to the Milky Way? What bodies would remain bound to an isolated star in the face of accelerated expansion? This paper develops both approaches — analytically in §2 and numerically in §3 — and elucidates the relationship between them. Our numerical simulations also show that the density profiles of dark matter halos approach a nearly universal form. Every dark matter halo grows asymptotically isolated and becomes the center of its own island universe; each of these regions of space-time then approaches a universal geometry. In §4, we determine the sphere of influence of existing structures and find the future time at which they grow cosmologically isolated. Next, we consider the implications of cosmic acceleration for the background radiation fields, suppression of particle annihilation, and the long term geometry of space-time. Because the equation of state of the dark vacuum energy is not completely determined, we generalize these results (in an Appendix) to consider dark energy that varies with time (equivalently, the scale factor).

2. ANALYTICAL DESCRIPTIONS OF STRUCTURE FORMATION

Before performing detailed numerical simulations of future structure formation, it is useful to develop simple analytical estimates. Such results have been developed previously to account for past structure formation in an accelerating universe (see especially Lokas & Hoffman 2001). While most past work has emphasized the evolution of structure up to the present epoch, we focus here on its evolution into the future. Throughout this treatment, we assume a spatially flat universe, which at the present epoch has $\Omega_{\rm m,0} = 0.3$ and $\Omega_{\rm v,0} = 0.7$ ($\Omega_{\rm m,0} + \Omega_{\rm v,0} = 1$). In the future, the values of $\Omega_{\rm m}$ and $\Omega_{\rm v}$ vary, but their sum continues to equal unity.

2.1. *Collapse of overdense regions*

The evolution of a given region of the universe is described by an energy equation. For a spherical patch of physical size r, this energy equation can be written in the form

$$\frac{1}{2}\dot{r}^2 - \frac{GM}{r} - \frac{1}{2}H^2 r^2 \Omega_{\rm v,0} = E\,, \qquad (1)$$

where the energy E is given by

$$E = \frac{1}{2}H_0^2 r_0^2 \big[1 - \Omega_{\rm m,0}(1+\delta_0) - \Omega_{\rm v,0}\big]\,. \qquad (2)$$

This set of equations implicitly assumes that $\dot{r} = H_0 r_0$, i.e., that the particles are traveling along with the unperturbed Hubble flow at the present epoch. Later in this section, we generalize this analysis to consider the case in which particles have already slowed down relative to the Hubble flow due to the past action of gravity.

If we define the dimensionless variable $\xi \equiv r/r_0$ and the dimensionless time $\tau \equiv H_0 t$, then the energy equation can be rewritten in the simpler form

$$\big(\frac{d\xi}{d\tau}\big)^2 = 1 + \Omega_{\rm m,0}\big(\frac{1}{\xi} - 1\big)(1+\delta_0) + \Omega_{\rm v,0}(\xi^2 - 1)\,. \qquad (3)$$

If a cosmological structure is slated to collapse in the future, then the effective velocity (the time derivative of ξ) must change sign, which requires the right hand side of the above equation to vanish. This requirement results in a cubic equation of the form

$$\xi^3 + \big[\frac{1}{\Omega_{\rm v,0}} - 1 - \frac{\Omega_{\rm m,0}}{\Omega_{\rm v,0}}(1+\delta_0)\big]\xi + \frac{\Omega_{\rm m,0}}{\Omega_{\rm v,0}}(1+\delta_0) = 0\,. \qquad (4)$$

For a given (flat) cosmology (a given value of $\Omega_{\rm m,0}$, which in turn specifies $\Omega_{\rm v,0} = 1 - \Omega_{\rm m,0}$), and a given overdensity δ_0, the cubic has three real roots if the following constraint is satisfied:

$$\big[\frac{\Omega_{\rm m,0}}{\Omega_{\rm v,0}}(1+\delta_0)\big]^2 < \frac{4}{27}\big[1 + \frac{\Omega_{\rm m,0}}{\Omega_{\rm v,0}}(1+\delta_0) - \frac{1}{\Omega_{\rm v,0}}\big]^3\,. \qquad (5)$$

The minimum overdensity δ_0 occurs when the above constraint is saturated (i.e., at equality). For a given value of $\Omega_{\rm m,0}$, the vacuum energy density $\Omega_{\rm v,0} = 1 - \Omega_{\rm m,0}$ is specified, and the equation has a given root. For the currently favored cosmological model with $\Omega_{\rm m,0} = 0.3$, the root occurs for $\delta_0 = 17.6$.

2.2. *Criterion for being bound to existing structures*

A related issue is to ask whether a small mass or test particle will be bound to currently existing cosmological structures. To carry out this calculation, we consider an existing object of mass $M_{\rm obj}$, which could be (the dark matter halo encompassing) a galaxy or a cluster of galaxies. We then ask whether test particles — much smaller structures exterior to the system — will be bound to $M_{\rm obj}$ or not. The test particles start with a radial distance r_0 at the present epoch. For simplicity, we assume that the distance r_0 is much larger than the size of the collapsed object so that the potential of a point mass provides a good approximation.

The calculation is analogous to that of the previous section, with the mass of the potentially collapsing system replaced by the mass $M_{\rm obj}$ of the pre-existing structure. The energy equation can again be written in non-dimensional form

$$\big(\frac{d\xi}{d\tau}\big)^2 = 1 + (\Omega_{\rm m,0} + \beta)\big[\frac{1}{\xi} - 1\big] + \Omega_{\rm v,0}(\xi^2 - 1)\,, \qquad (6)$$

where we have defined

$$\beta \equiv \frac{2GM_{\rm obj}}{H_0^2 r_0^3}\,. \qquad (7)$$

The parameter β thus measures the effective "strength" of the galaxy or cluster. The requirement that equation (6) have a turnaround point leads, as before, to a cubic constraint, which now takes the form

$$\Omega_{\rm v,0}\xi^3 - \beta\xi + (\Omega_{\rm m,0} + \beta) = 0\,, \qquad (8)$$

which in turn requires

$$\beta^3 \geq \frac{27}{4}(\Omega_{\rm m,0} + \beta)^2\,\Omega_{\rm v,0}\,. \qquad (9)$$

The minimum value of the strength parameter occurs when the equality is saturated and we denote the corresponding value of β by $\beta^\star$. Solving equation (9), we find the value $\beta^\star \approx 5.3$. We can thus determine the condition that must be met in order for a test body to remain bound to an object of mass $M_{\rm obj}$, i.e.,

$$2GM_{\rm obj} \geq \beta^\star H_0^2 r_0^3\,. \qquad (10)$$

Inserting numerical values and scaling the result, we thus obtain the following criterion

$$\frac{M_{\rm obj}}{10^{12} M_\odot} > 3\, h_{70}^2 \left(\frac{r_0}{1\,{\rm Mpc}}\right)^3 , \qquad (11)$$

where we have defined $h_{70} \equiv H_0/(70\ {\rm km\ s^{-1}\ Mpc^{-1}})$.

As an immediate application of the above result (eq. [11]), we can determine whether or not the Milky Way (Local Group) will remain bound to the Virgo cluster in our cosmological future. The mass of Virgo is estimated to be $M_{\rm Virgo} = 5\times10^{13} - 10^{14}\ M_\odot$ and its current distance from the Milky Way is about $r_0 = 16$ Mpc (e.g., Jacoby et al. 1992). The requirement specified by equation (11) is not met — the mass falls short by a factor of 100 — so that the Milky Way is not destined to be bound to Virgo. This result is verified by numerical simulations (see §2 and Nagamine & Loeb 2002).

Equation (11) thus defines an effective sphere of influence for any given astronomical object — when considered as isolated in a background universe dominated by a cosmological constant. For our Milky Way galaxy, this sphere has radius $r_0 \approx 0.7$ Mpc. For an isolated star (i.e., a free-floating star not associated with a galaxy), with typical stellar mass $M_* = 0.5\ M_\odot$, the sphere of influence has size $r_0 \approx 55$ pc. This size scale suggests that isolated binary star systems can remain safely bound. Although isolated pairs of galaxies can also remain gravitational bound, they live much closer to the brink of instability.

The above analysis finds the sphere of gravitational influence for test bodies that are moving along with the Hubble flow at the present epoch. However, due to the past evolution of the universe, bodies that are now outside galaxies (or clusters) can be slowed down relative to the Hubble flow due to the action of gravity in the past. In particular, the particles simulated in N-body simulations can be slowed down relative to the Hubble flow. To include this effect in the analysis, we modify equation (6) to take the new form

$$\left(\frac{d\xi}{d\tau}\right)^2 = A + (\Omega_{\rm m,0} + \beta)\left(\frac{1}{\xi} - 1\right) + \Omega_{\rm v,0}(\xi^2 - 1)\,, \qquad (12)$$

where the constant A represents the fact that the test particles have been slowed down relative to the Hubble flow (and rest of the quantities are the same as in eq. [6]). The value $A = 1$ corresponds to particles moving with the Hubble flow, so that particles that have been slowed will have $A < 1$. The case $A = 0$ provides a benchmark, where test bodies have zero velocity (are turning around) at the present epoch.

The requirement that equation (12) have a turnaround solution implies a modified form of equation (9), namely,

$$(\beta + 1 - A)^3 \geq \frac{27}{4}\Omega_{\rm v,0}(\Omega_{\rm m,0} + \beta)^2\,. \qquad (13)$$

By solving the above cubic for a given A when the inequality is saturated, we find the root $\beta^\star(A)$ that can be used to define the sphere of influence of a given cluster or galaxy according to equation (10). For the benchmark case, $A = 0$, the root $\beta^\star \approx 1.1$, and hence the effective sphere of influence is larger than the previous case by a factor of 1.7.

In the following section, we compare these analytic predictions to the results of numerical simulations. If we insert test bodies at the present epoch — at rest with respect to the Hubble flow — then the sphere of gravitational influence of existing structures is described accurately by equation (11). In addition, although mass particles that begin at rest (with respect to the Hubble flow) in the distant past are slowed down and have values $A < 1$ at the present epoch, the prediction of equation (11) works respectably well (see the following section).

3. NUMERICAL SIMULATIONS OF STRUCTURE FORMATION

To evaluate the analytic results of the previous section, particularly equation (11) defining the gravitational sphere for influence for an object of mass M, we have run a series of numerical simulations of the evolution of structure in a Λ-dominated universe into the future. All simulations were run using the GADGET code (Springel, Yoshida, & White 2001)[2] on a parallel computer cluster at Michigan's Center for Advanced Computing. A flat ΛCDM model is assumed, with matter density $\Omega_{\rm m,0} = 0.3$, power spectrum normalization $\sigma_8 = 1.0$, and $h = 0.7$, where the Hubble parameter $H_0 = 100h\,{\rm km\,s^{-1}\,Mpc^{-1}}$. The simulations followed the evolution of a 256.48 h^{-1}Mpc region with 128^3 dark matter particles of mass $6.70\times10^{11}h^{-1}M_\odot$, starting from $a = 0.258$ ($z = 20.8$), through the present, and forward to $a = 100$. A gravitational force softening of $200h^{-1}$kpc (in physical units) was used throughout the computation.

In addition to the simulation described above, which was evolved to a=100, we performed a similar simulation that evolved the $a = 1$ configuration forward with an added set of initially stationary test particles. In this run, 96 particles were placed in a spherically symmetric fashion around the centers of 19 dark matter halos. In each case, they were placed at rest on one of 12 concentric spheres centered at the most bound position of the selected group. This simulation was also evolved to $a = 100$.

The top two panels of Figure 1 show structure in a fixed comoving region 128 h^{-1} Mpc wide by 25 h^{-1} Mpc deep at (a) the present epoch and (b) $a = 100$. The large-scale pattern of the cosmic web is well established by $a = 1$ and evolves little thereafter (as emphasized by Nagamine & Loeb 2002). Clusters of fixed physical size shrink as $1/a$ in the comoving frame, so the halo population effectively condenses into a sea of "droplets" embedded in the frozen linear modes that define the filaments, walls, and voids that characterize the cosmic structure today.

Panels (c) and (d) change perspective by showing how the physical region of panel (a) appears at $a = 11$ and $a = 100$, respectively. The physical separation between bound structures grows exponentially in time during the deSitter expansion phase of the dark energy dominated era. The future is increasingly lonely.

To compute the size of a bound halo — its gravitational sphere of influence defined in the previous section — we identify the smallest radius at which the local mean radial velocity is significantly larger than zero. We measure such sizes using two different tracers: the simulation particles themselves or the test particles of the second simulation. Since the latter are embedded at rest at $a = 1$, their future evolution should better follow, within the limits provided by a monopole description of gravity, the prediction

[2] http://www.MPA-Garching.MPG.DE/gadget/

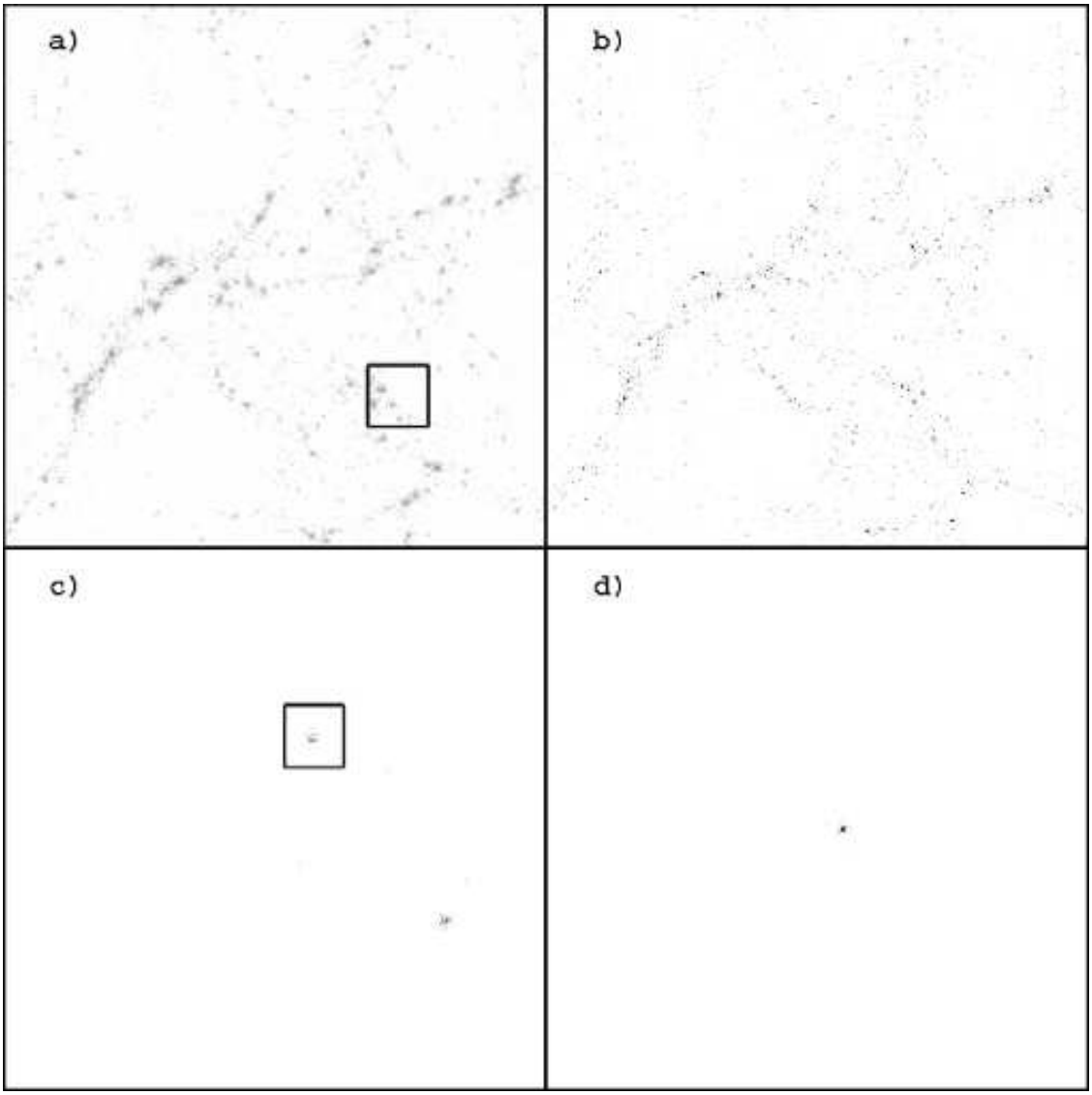

FIG. 1.— Evolution of structure in a Λ-dominated universe. Panels a) and b) show snapshots of a comoving region of the universe 128 h^{-1} Mpc on a side and 25 h^{-1} Mpc thick today ($a = 1$) and at cosmic age 91.5 Gyr in the future ($a = 100$), respectively. Panels c) and d) show regions of the same *physical* size as that shown in panel a) at epochs $a = 11$ and $a = 100$, respectively. The box in panel a) locates the region shown in b), and the box in panel c) locates the region shown in d).

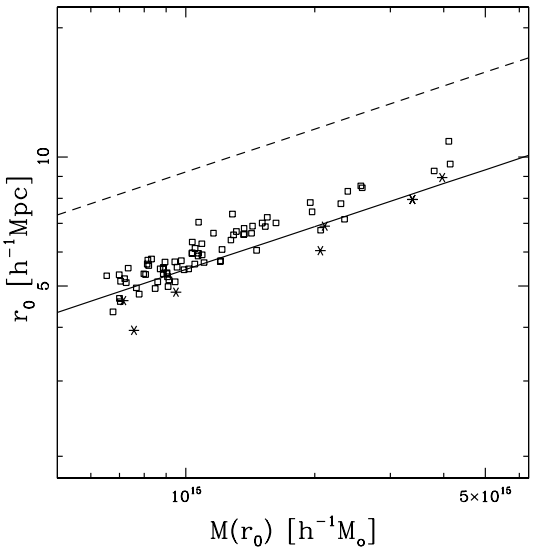

FIG. 2.— Gravitational sphere of influence of a cosmological object, as a function of the mass enclosed within the sphere of influence at a=1. The lower solid line marks the analytic prediction for objects starting at rest with respect to the Hubble flow (eq. [11]); the upper dashed line marks the analytic prediction for objects that are at rest relative to the cluster at the present epoch (i.e., objects that are marginally separated from the Hubble flow — see eq. [12]). These analytic predictions are compared with simulations, both for cluster particles (open squares) and for the test particles placed in the simulation at rest (stars).

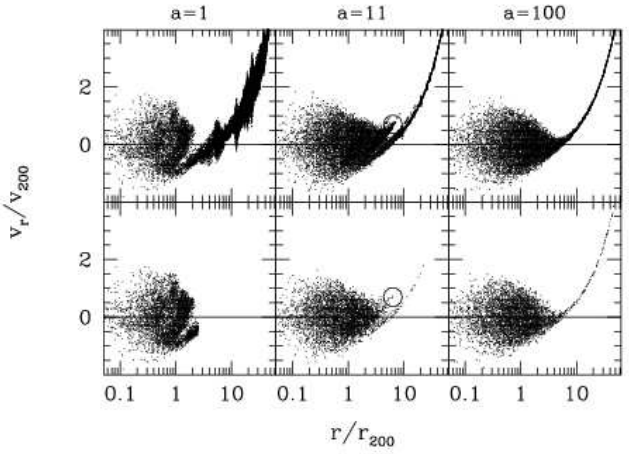

FIG. 3.— Radial velocity relative to the cluster center as a function of distance for particles in the largest halo at the epochs indicated. The upper panel shows all matter while the lower panel shows only those particles that lie within $2.5r_{200}$ at $a = 1$.

of equation (11) which assumes a pure, spherical Hubble flow.

Measurements of the gravitational sphere of influence are shown in Figure 2. Note that the relevant mass is the mass within the sphere of influence at the present epoch; this is typically a factor of 2–3 larger than M_{200}. The relation between this mass and its sphere of influence for test particles placed in the simulation at rest at $a = 0$, shown as stars, is in excellent agreement with the predictions of equation (11), shown as the lower line in the figure. Values for the simulation particles, shown as open squares, are slightly larger (by about 10%) because radial infall in the weakly non-linear regime reduces the kinetic energy associated with Hubble flow. These sizes are bounded from above by the modified relation, equation (12), with $A = 0$, shown as the upper dashed line in the figure.

3.1. *Halo Phase-space Structure*

In the far future, the character of halos' radial phase-space structure is markedly different from that of today. The upper row of Figure 3 shows the radial velocity pattern of the most massive halo at $a = 1$, 11 and 100. The halo identified at present remains the most massive at all future times. At each epoch, lengths are expressed in units of r_{200}, the radius within which the mean enclosed density is 200 times the critical value. Physical velocities are expressed in units of $v_{200} = \sqrt{GM_{200}/r_{200}}$, where M_{200} is the mass within r_{200}. The halo's physical size grows from $M_{200} = 1.08 \times 10^{15} h^{-1}\mathrm{M}_\odot$ at $a = 1$ to $2.35 \times 10^{15} h^{-1}\mathrm{M}_\odot$ at $a = 11$, and remains nearly constant thereafter.

At $a = 1$, positive velocity particles at radii $r/r_{200} \sim 1-2$ represents material that has penetrated the halo core and is streaming outward to large radii. This "processed" material mixes at these radii with a fresh stream infalling at $v_r \simeq -v_{200}$. The stream extends outward through a zero-velocity surface at $r \simeq 5r_{200}$, and asymptotically approaches the Hubble flow at large radii. The present-epoch interior phase structure displays a lumpy morphology, evidence of recent merger activity that has not yet dynamically relaxed. The infall pattern shows spikes of enhanced dispersion, the signatures of neighboring halos. Those within the gravitational sphere of influence are destined to merge with the central halo.

By $a = 11$, phase mixing has smoothed the interior structure considerably, but the remains of a recent merger can be seen in a small tail of outflow centered at $r/r_{200} \sim 6$ (circled in the panel). The infall regime is much quieter, with only a few collapsed structures evident in the tail of Hubble flow. At $a = 100$, the interior phase structure is extremely homogeneous and the infall regime is essentially silent; no collapsed structures perturb the flow within $50r_{200}$.

The lower panels of Figure 3 show how the non-linear material of the present cluster evolves into the future. Only those particles lying within $2.5r_{200}$ at $a = 1$ are shown. This radius is chosen to encompass all the "processed" halo material at the present epoch. Although this boundary extends beyond most common choices for the

"virial radius" of a halo (Evrard, Metzler & Navarro 1996; Eke, Cole & Frenk 1996; White 2001), it is evident that some material currently within this radius is destined for future escape. A thin tail forms of material lifted off the halo, representing 0.8 and 2.6 percent (at $a = 11$ and 100, respectively) of the mass within $2.5r_{200}$ at $a = 1$. Note that the merger system at $a = 11$ circled in the upper panel is not as strongly evident in the lower panel, indicating that it lies beyond $2.5r_{200}$ at the present epoch.

The simple, smooth phase structure at late times suggests a long-term equilibrium. In the next subsection, we address the question of the eventual shape of the radial mass profiles of halos.

3.2. *Halo Density Profile*

Numerical studies have revealed that the non-linear density structure of halos formed through gravitational clustering takes on a common form. The first such studies (Navarro, Frenk & White 1996; 1997) showed that this density profile can be written in the form

$$\rho(r) = \frac{4\rho_s}{r/r_s[1+(r/r_s)]^2}\,, \qquad (14)$$

where r_s is a characteristic radius where the logarithmic slope of the density profile is isothermal: $\mathrm{d}\ln\rho/\mathrm{d}\ln r = -2$. The ratio r_{200}/r_s defines the concentration parameter c. Note we have chosen the convention $\rho_s = \rho(r_s)$; in this case the inner density can be directly related to the concentration of an NFW profile via

$$\rho_s = \frac{1}{4}\delta_c\rho_{\rm c} = \frac{\Delta}{12}\frac{c^3}{\ln(1+{\rm c}) - {\rm c}/(1+{\rm c})}\rho_{\rm c}. \qquad (15)$$

Previous fits to this density profile have been limited to radii $r \lesssim r_{200}$ and epochs $a \leq 1$. We present here an extension of this form to larger radii and future epochs.

Figure 4 shows radial density profiles derived from stacking the 50 most massive halos at each epoch displayed. Solid lines in the figure show binned profiles for five epochs from $a = 1--100$, while dashed lines show fits to the form

$$\rho(r) = \frac{A\rho_s}{r/r_s[1+(r/r_s)^p]^{3/2}}[1+r/r_\infty]^{1+3p/2}\,. \qquad (16)$$

Here r_s is a scale radius similar to the that of equation (14), r_∞ is an asymptotic radius, p is a free parameter and $A = 2^{3p/2}/[1+r_s/r_\infty]^{1+3p/2}$. We find that values $p = 1.8$, $r_s = 0.50$ and $r_\infty = 4.7r_{200}a^{6/(3p+2)}$ provide fits that are accurate to $\langle(\delta\rho/\rho)^2\rangle^{1/2} \sim 35\%$ over the full range of radii and epochs examined. The scaling of r_∞ with expansion factor ensures that the profile approaches the mean mass density of the universe as $r \to \infty$.

The profile of equation (16) is steeper than the NFW form at radii beyond r_{200}. As $r_\infty \to \infty$, the logarithmic slope of the profile well beyond r_{200} approaches 3.7 (shown by the dot-dashed curve in Figure 4), steeper than the slope of 3 from the NFW case. This difference in slope keeps the enclosed mass from being logarithmic divergent, as implied by a formal extrapolation of the NFW form (compare eq. [14] with [16]).

In fact, the mass of a halo in the far future will be simpler to define than it is today. At present, radial infall and incomplete dynamical relaxation make the choice of the "edge" of a cluster somewhat arbitrary (White 2001; Evrard & Gioia 2002). In the relatively near future, however, halos evolve toward an equilibrium configuration that is bounded by an increasingly sharp zero-velocity surface (Figure 3). Ultimately, a meaningful and unique definition of mass emerges, namely, all of the matter lying interior to this well-defined zero-velocity surface. In addition, as shown by Figure 4, the density profile attains a well-defined form.

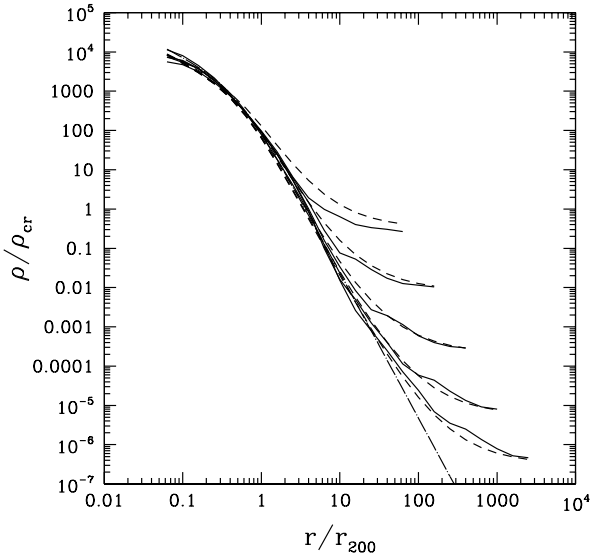

FIG. 4.— The asymptotic form for the density distribution of dark matter halos. The solid curves show the (nearly) universal form for dark matter halos, for a variety of epochs (from top to bottom, $a =$ 1, 3.38, 11.4, 38.6, and 100). Starting just after the present time, the dark matter halo profiles show essentially the same form, only the outer boundary is stretched to match onto the ever-lower density of the background universe. The dashed curves show the fit to the numerical results, equation (16), evaluated at each epoch with the parameters given in the text. The dot-dashed curve shows the asymptotic form of the density profile in the limit $t \to \infty$.

4. LONG-TERM RAMIFICATIONS OF COSMIC ACCELERATION

The considerations of the previous sections outline the requirements necessary for future structure formation and the criteria for test bodies to remain bound to existing astronomical structures. With these results in place, we can fill out the picture of the future evolution of our cosmos. In particular, we can determine the time scales for various bound structures to grow isolated, the corresponding effects on the background radiation fields in the universe, and the freezing out of particle annihilation processes.

4.1. *Isolation of bound structures*

Because our universe contains a dark vacuum component, it has a well-defined horizon scale. For unbound objects living in this accelerating universe, the next issue is thus to determine when the objects leave the horizon. The background universe can be described by its line element, which can be written in advanced time coordinates in the form

$$ds^2 = -\left[1-\chi^2r^2\right]dv^2 + 2dvdr + r^2d\Omega^2\,. \qquad (17)$$

This line element ignores the curvature due to gravitationally-condensed structures (see the following subsection). The parameter χ is related to the magnitude of the cosmological constant and is defined by the relation (in natural units)

$$\chi = \Big(\frac{2\pi^3}{45}\Big)^{1/2} \frac{\Lambda^2}{M_{\rm pl}}\,, \tag{18}$$

where Λ is the effective temperature scale of the cosmological vacuum energy ($\Lambda \approx 0.003$ eV ≈ 35 K for the presently suspected cosmological constant). In such a universe, the horizon distance r_H is given by

$$r_H = \chi^{-1} = \frac{c}{H_0}\frac{2}{\pi}\Big(\frac{15}{\Omega_{\rm v,0}}\Big)^{1/2} \approx 12,600 \text{ Mpc}\,, \tag{19}$$

where the second equality assumes the standard values $\Omega_{\rm m,0} = 0.3$ and $\Omega_{\rm v,0} = 0.7$. This horizon distance r_H is not the same as the particle horizon, but rather is essentially the Hubble radius. This distance scale r_H provides an effective "boundary for microphysics" within the much larger space-time of the universe (for further discussion of horizons, see Kolb & Turner 1990 and Ellis & Rothman 1993).

For a flat universe with both matter and vacuum components, the scale factor $a(t)$ increases according to the function

$$a(t) = \Big(\frac{\Omega_{\rm m,0}}{1-\Omega_{\rm m,0}}\Big)^{1/3} \Big\{\sinh\big[\frac{3}{2}\sqrt{1-\Omega_{\rm m,0}}\,H_0 t\big]\Big\}^{2/3}. \tag{20}$$

At later times, the scale factor approaches the simpler asymptotic form

$$a_{\rm asym}(t) = \big(\frac{\Omega_{\rm m,0}}{4\Omega_{\rm v,0}}\big)^{1/3} \exp[\sqrt{\Omega_{\rm v,0}}\,H_0 t]\,. \tag{21}$$

One can see immediately that the e-folding time scale of the future universe is $\tau_e = \Omega_{\rm v,0}^{-1/2} H_0^{-1} \approx 17$ Gyr. Furthermore, the scale factor $a(t)$ approaches this asymptotic form on an even shorter time scale. If the full expression (eq. [20]) is written as the asymptotic form (eq. [21]) plus correction terms, those correction terms decay with a time scale $\tau = (3H_0\sqrt{\Omega_{\rm v,0}})^{-1} = \tau_e/3 \approx 5.6$ Gyr. This time scale — somewhat longer than the age of the solar system and appreciably younger than the current age of the universe — is a direct manifestation of the cosmological constant problem.

Given that any extant cosmic structure has a sphere of influence (eq. [11]) and that the universe has a fixed horizon size r_H, every structure will become isolated when the radius of its sphere of influence is stretched beyond the horizon, i.e., when $a(t)r_0 > r_H$. For a structure of mass $M_{\rm obj}$, isolation occurs at a time $t_{\rm iso}$ given by

$$t_{\rm iso} = \frac{2}{3}\tau_e \sinh^{-1}\left\{\Big[\frac{4\beta^\star(15)^{3/2}}{\pi^3}\frac{c^3\tau_e}{GM_{\rm obj}\Omega_{\rm m,0}}\Big]^{1/2}\right\}. \tag{22}$$

As a result, for vast majority of cosmological time, the cosmos will be divided into "island universes" in the sense that bound clusters of galaxies will retain their sizes (a few to several Mpc) while the distance between clusters grows exponentially (see also Chieuh & He 2002). Given typical cluster sizes and separations, we predict that clusters will grow isolated in about 120 Gyr. For the particular values appropriate for the nearby Virgo cluster, equation (22) implies an isolation time of 132 Gyr (this time is the age of the universe at the time of isolation; since the universe is already about 14 Gyr old, this event will occur 118 Gyr from now). Structures with lower mass have smaller spheres of gravitational influence and require longer times to grow isolated. Our local group, with an estimated mass of $M_{LG} \approx (2.3 \pm 0.6) \times 10^{12}\ M_\odot$ (van den Bergh 1999), will be isolated at cosmic age $t = 175$ Gyr. As another example, a star that is not gravitationally bound to a larger structure (e.g., one that has been scattered out of a galaxy) requires somewhat longer to become isolated — about 336 Gyr. For comparison, the lifetimes of the smallest, longest-lived stars are measured in tens of trillions of years (Laughlin, Bodenheimer, & Adams 1997; hereafter LBA97), about one hundred times longer than the isolation time for galaxy clusters. For most of eternity, and indeed for most of the Stelliferous Era, clusters will be alone. Inside the galaxies, the expansion has essentially no effect, and star formation and stellar evolution continue for trillions of years (AL97). When viewed on the large scale, however, these clusters will behave like point sources, pumping radiation into an ever-expanding void.

4.2. *Asymptotic structure of space-time*

In the long term, existing cosmic structures will remain bound, but will grow isolated. These structures will be embedded within an accelerating universe with a constant horizon scale (eq. 19). This process effectively divides the present-day universe into many smaller regions of space-time. These "island universes" display properties of a universal nature.

Every given "island universe" will approach a fixed overdensity. The energy density contained with the horizon scale is equivalent to a mass M_H given by

$$M_H = \frac{4\pi}{3}\rho_{V(t\to\infty)}\, r_H^3 = \frac{\Omega_{\rm v,0}}{2GH_0}\Big(\frac{2c}{\pi}\Big)^3\Big(\frac{15}{\Omega_{\rm v,0}}\Big)^{3/2} \approx 8\times 10^{23} M_\odot\,. \tag{23}$$

Since the mass contained within any given isolated cluster will be constant, the overdensity approaches a constant value. For our particular environment, the local group will remain bound with its mass of about $M_{LG} = 2.3\ \times 10^{12}\ M_\odot$. The mass in our local region is thus destined to be a minor perturbation on the cosmos itself, even within our local island universe. For cosmic ages older than 175 Gyr, the mass contribution to the universe contained within the local group is given by $\delta_\infty = M_{LG}/M_H \approx 3\times 10^{-12}$, only 3 parts per trillion.

Our numerical simulations indicate that cosmic structures, from galaxies to clusters, tend to develop universal forms for their density profiles. As a result, every island universe will attain the same general form for its space-time. In particular, since the density profile attains the universal form described by equation (16), the line element ds^2 for the space-time within the horizon distance r_H also attains a universal form. If we take the center of the coordinate system to be the center of the cluster and assume that the mass distribution is spherically symmetric, the line element can be written in the form

$$ds^2 = -\Big(1 - A(r) - \chi^2 r^2\Big)dt^2 + \Big(1 - B(r) - \chi^2 r^2\Big)^{-1} dr^2 + r^2 d\Omega^2\,, \tag{24}$$

where $A(r)$ and $B(r)$ depend on the mass distribution (see, e.g., Misner, Thorne, & Wheeler 1973). This form for the line element is that of a mass distribution embedded in de-Sitter space (see also Bardeen 1981, Mallet 1985, Chiueh & He 2002). As a result, there exists an outer horizon at $r = \chi^{-1}$. We provide a more detailed specification of the metric in a future work (Adams et al 2003).

The outer horizon supports the emission of radiation through a Hawking-like mechanism (e.g., Fulling 1977, Birrell & Davies 1982). As a result, the universe will be filled with a nearly thermal bath of radiation with characteristic wavelength $\lambda \sim r_H \sim \chi^{-1} \sim 12,600$ Mpc and characteristic temperature $T \sim \chi \sim \Lambda^2/M_{\rm pl} \sim 10^{-33}$ eV $\sim 10^{-29}$ K. This bath of radiation will become the dominant background radiation field at very late times (after about one trillion years – see the following section).

4.3. *Background radiation fields in an accelerating universe*

As the universe expands, all radiation fields are redshifted to longer wavelengths. An important milestone is reached when the typical wavelength of a given radiation field grows longer than the cosmological horizon scale defined by equation (19). After this crossing, the photons are larger than the largest "box" that the universe has to contain them. For later times, it no longer makes sense to describe the photons in terms of a distribution function. Inside the horizon, in the limit $\lambda \gg r_H$, the background photons will appear as "slowly" varying electric fields rather than as particles of light. The dominant background radiation field will be that produced by the horizon itself through a Hawking-like mechanism (see §4.2, Fulling 1977, Birrell & Davies 1982).

Given the scale factor of the universe and the present day wavelength of a radiation field, it is straightforward to find the time at which the photons are stretched beyond the horizon scale, i.e., when $\lambda a(t) > r_H$. For the cosmic background radiation, the present day wavelength (at the peak of the distribution) is about $\lambda_0 = 0.1$ cm and the photons cross the horizon at a time of 1120 Gyr.

The cosmic background photons are stretched beyond the horizon well before the stars stop shining. Star formation and stellar evolution will continue until the universe is tens of trillions of years old (AL97, LBA97). Suppose that stars continue to shine for 10 trillion years. By this late epoch, most of the remaining stars will be red dwarfs that emit light with a characteristic wavelength of $\lambda = 1$ μm $= 10^{-4}$ cm. If this red light is emitted up to a time t_* ($\approx 10^{12}$ yr) and observed at a later time t, its observed wavelength is given by

$$\lambda_{\rm obs} = \lambda_{\rm emit} \frac{a_{\rm obs}}{a_{\rm emit}} = \lambda_{\rm emit} \exp\left[(t - t_*)/\tau_e\right], \qquad (25)$$

where $\tau_e = 17$ Gyr is the e-folding time of the future universe. Starlight leaves the horizon when $\lambda_{\rm obs} > r_H$. Using this criterion in conjunction with equations (19) and (20), we find that starlight is redshifted out of the horizon over a time interval of only $\Delta t = (t - t_*) = 1260$ Gyr. Stellar evolution times — for the smallest stars — are much longer than the cosmological expansion times, so that photons are rapidly stretched beyond the horizon. Specifically, this stretching time is a small fraction of the Stelliferous Era, the time over which the universe will contain substantial numbers of hydrogen burning stars, i.e., $\Delta t/t_* \approx 10^{-2}$.

4.4. *Particle annihilation in an accelerating universe*

For material between galaxies — particles that are not bound to large structures — future evolution can continue through particle annihilation. The number density n of a given particle species is given by the evolution equation

$$\frac{dn}{dt} + 3Hn = -\langle \sigma v \rangle n^2 , \qquad (26)$$

where $\langle \sigma v \rangle$ is the appropriate average of the interaction cross section and the relative velocity (see, e.g., Kolb & Turner 1990; see also Cirkovic & Samurovic 2001). For an accelerating universe with a cosmological constant, the solution to equation (26) can be found and written in terms of the scale factor, i.e.,

$$n(a) = n_0 a^{-3} \left\{ 1 + \frac{2\Gamma}{3\Omega_{\rm m,0}} \left[1 - \sqrt{\Omega_{\rm v,0} + \Omega_{\rm m,0} a^{-3}} \right] \right\}^{-1} , \qquad (27)$$

where n_0 is the particle density at the present epoch and where we have defined $\Gamma \equiv \langle \sigma v \rangle n_0 / H_0$. The leading factor ($a^{-3}$) represents the dilution of the number density due to cosmic expansion, whereas the second factor in brackets incorporates the effects of continued particle annihilation. In an accelerating universe, annihilation is highly suppressed. For example, in the asymptotic limit $t \to \infty$, $a \to \infty$, this factor becomes $\mathcal{F} = 1 + 2\Gamma(1 - \sqrt{\Omega_{\rm v,0}})/3\Omega_{\rm m,0}$ $\approx 1 + 0.0048\ [\langle \sigma v \rangle / {\rm barn} \cdot c]$. For electron-positron annihilation, for example, the maximum correction term is less than a percent. For annihilation of cold dark matter particles (thought to be the dominant matter contribution), the interaction cross sections typically lie in the range $\sigma \sim 10^{-12} - 10^{-14}$ barn (e.g., Kolb & Turner 1990) and the speed $v/c \sim 10^{-3}$. As a result, the already small correction term (0.0048) is suppressed by an additional 16 orders of magnitude. This enormous suppression is driven by the relentless expansion of an accelerating universe.

When the number density grows so diffuse that the universe contains less than one particle per horizon volume, then individual particles are effectively isolated. The condition for such isolation can be written in the form

$$a(t) > \left(\frac{4\pi}{3} n_0 \right)^{1/3} r_H , \qquad (28)$$

where the scale factor a is given by equation (20) and the horizon scale is given by equation (19). Adopting a present day number density of $n_0 = 10^{-6}$ cm^{-3} results in a particle isolation time scale of about 1060 Gyr.

5. DISCUSSION AND CONCLUSIONS

This paper explores the future evolution of a universe dominated by dark vacuum energy. Analytic estimates are compared to results of numerical simulations that follow the evolution of future structures in such an accelerating universe.

For a universe with cosmological constant $\Omega_{\rm v,0} = 0.7$, only those regions with present-day overdensities $\delta_0 > 17.6$ will remain gravitationally bound, in agreement with earlier estimates (Lokas & Hoffman 2002; Nagamine & Loeb 2003). We generalize this result to include quintessence models with constant forms for the equation of state (Appendix A). We have also derived the condition required for

test bodies to remain bound to existing structures (see eq. [11]) and verified its validity with numerical simulations (to within $\sim 10\%$; see Figure 2). Any collapsed object — from a star to galaxy cluster — has a finite sphere of gravitational influence in an accelerating universe, with radius $r_0 \approx 1$ Mpc $(M_{\rm obj}/10^{12}M_\odot)^{1/3}$. For quintessence models, we have derived an analogous result for the sphere of gravitational influence (see Appendix A and eq. [A7]).

From a co-moving perspective, the large-scale appearance of the future universe is little changed from that of today. Matter in the cosmic web drains efficiently into collapsed halos that shrink in comoving coordinates. The halos are essentially frozen in place while their contrast relative to the mean background grows with time. In physical coordinates, the view is rather different. The vast majority of the galaxies now visible are pulled out of the immediate horizon of any given bound structure (a cluster or group). In the long term, only the cluster or group itself remains within the effective horizon scale of $r_H = 12{,}600$ Mpc.

The long-term structure of space-time consists of a flat metric dimpled with isolated clusters that approach a fixed mass profile. We find that halo density profiles approach a form similar to, but steeper at large radii than, the NFW profile (equation [16]). It is important to emphasize that *every* halo grows isolated in the long term, i.e., every gravitationally bound mass concentration ultimately becomes the only structure within its own island universe. In each such local region, the halo density takes the form shown in Figure 4 and the line element of the space-time metric takes the form given by equation (24). Although the halo mass varies from region to region, the form of the metric – and hence the geometry of space-time – is nearly universal. In all cases, the halo mass in any region provides only a minor contribution to the overall mass/energy budget, with $M_{\rm obj}/M_H \sim 10^{-11}$.

As the universe continues to expand, and accelerate, cosmic radiation fields are redshifted to increasingly long wavelengths. After about one trillion years, the cosmic background radiation (leftover from the big bang) is stretched beyond the horizon and the dominant radiation background is that emitted by the horizon itself through a Hawking-like mechanism. Many of the results of this investigation can be summarized in terms of the relevant time scales, which are listed in Table 1. To emphasize the mismatch between the various time scales, the table also lists the scale factor for each relevant epoch. For example, individual stars grow isolated in 336 Gyr ($a = 2 \times 10^8$), but the longest-lived stars burn hydrogen for 17,000 Gyr (when $a = 10^{434}$).

With the analysis complete, many of the time scales and length scales of the future universe can be understood in simpler terms. A dimensional analysis – presented in Appendix B – shows that the most important time scale is given by the asymptotic form for the Hubble parameter $H_\infty = \sqrt{\Omega_{\rm v,0}}H_0 \approx 59$ km s^{-1} Mpc^{-1}. The accelerated expansion itself completely dominates the evolution of the universe as a whole, so that all of the time scales are determined by $H_\infty^{-1} \approx 17$ Gyr and logarithmic multiplying factors (see Appendix B). By comparison, time scales for stellar evolution ($10^{13} - 10^{14}$ yr; AL97, LBA97) and dynamical relaxation of galaxies (10^{20} yr; BT87) are much longer.

The authors would like to thank Greg Laughlin for useful discussions. This work was supported by the University of Michigan through a Regents Fellowship (MTB), a Physics Department Fellowship (RHW), by the Michigan Center for Theoretical Physics, and by NASA Astrophysics Theory Grant NAG5-8458.

APPENDIX

A. QUINTESSENCE

In this Appendix we generalize our results to the case of a vacuum energy that depends on time, or equivalently, the scale factor a. For the sake of definiteness, we adopt the standard form for the vacuum energy equation of state, i.e., the vacuum pressure is given by

$$p_{\rm vac} = w\rho_{\rm vac}\,, \tag{A1}$$

where the parameter w is constant and lies in the range $-1 \le w < 0$. Current observations seem to indicate a somewhat smaller range $-1 < w \lesssim -0.5$ (e.g., Limin et al. 2000, Balbi et al. 2001). In fact, Spergel et al (2003) place a 95% confidence limit of $w \le -0.5$ using a combination of the WMAP CMB data and the HST key project (Freedman et al. 2001) value for the Hubble constant and find that $w \le -0.78$ when additional constraints are added (from the SNIa-derived redshift distance relation, the 2dFGRS large-scale structure, and Lyman-α data, assuming a flat universe with constant w). For completeness, we consider here the full range of constant w values from 0 to -1. With this equation of state, the scale factor evolves according to

$$\left(\frac{\dot a}{a}\right)^2 = H_0^2\Big\{\Omega_{\rm m,0}a^{-3} + \Omega_{\rm v,0}a^{-p}\Big\} \tag{A2}$$

where the index $p = 3(1+w)$.

The energy equation (6) that determines whether or not overdense regions collapse, and the fate of test bodies, can be written in the form

$$\big(\frac{d\xi}{d\tau}\big)^2 = \Omega_{\rm v,0}a^{-p}\xi^2 - \beta + (\Omega_{\rm m,0} + \beta)/\xi\,, \tag{A3}$$

where β measures the gravitational influence of an existing structure according to equation (7). The case of overdense regions can be considered by replacing β with $\Omega_{\rm m,0}\delta_0$, where δ_0 is the overdensity.

Table 1
Time Scales and Scale Factors

Event	*Time* τ (Gyr)	$a(\tau)$
Time scale for scale factor to approach exponential form	5.6	–
Inverse Hubble constant H_0^{-1}	14	–
e-folding time of the future universe $(H_0\sqrt{\Omega_{\rm v,0}})^{-1}$	17	–
Current age of the universe	13.7	1
Virgo Cluster leaves our horizon	132	1000
The Local Group grows isolated	180	2×10^4
Exiled stars become isolated	336	2×10^8
Individual particles grow isolated	1060	6×10^{26}
CBR photons stretch beyond the horizon	1120	2×10^{28}
Optical photons stretch beyond the horizon	1260	10^{32}
Lifetime of longest-lived stars	17,000	10^{434}
End of the Stelliferous Era	100,000	10^{2554}

In order to determine whether trajectories turn around (and hence remain bound or collapse), the right hand side of equation (A3) must vanish as before. In this case, however, the resulting cubic equation has time dependent coefficients and so the evolution of the scale factor must be considered simultaneously. As a result, we combine the two equations by changing the independent variable to a and thereby obtain

$$\left(\frac{d\xi}{da}\right)^2 = \frac{\Omega_{\rm v,0}a^{-p}\xi^2 - \beta + (\Omega_{\rm m,0}+\beta)/\xi}{a^2\left[\Omega_{\rm m,0}a^{-3} + \Omega_{\rm v,0}a^{-p}\right]}\,. \tag{A4}$$

Trajectories turn around when the right hand side of this equation vanishes. The minimum value of β required for such turnaround occurs when the right hand side of the equation has a double zero (both the right hand side and its derivative with respect to ξ vanish). To find the critical value of β, denoted here as $\beta^\star$, we numerically integrate equation (A4) and iterate to find the value that provides a double zero. This procedure must be carried out for every value of w (or p). The resulting values of β are given below. The overdensities required for the collapse of future structures, for a cosmology with a given value of w, are given by $\delta_0 = \beta^\star/\Omega_{\rm m,0}$. This quantity is shown in Figure A5.

We also provide a simple fit to the numerical result:

$$\beta^\star(w) = \beta_0^\star\left[1 + a(1+w) + b(1+w)^2 + c(1+w)^3\right], \tag{A5}$$

where $\beta_0^\star$ is the value for a cosmological constant ($\beta_0^\star \approx 5.3$; §3.2) and where the coefficients are given by

$$a = -2.33, \qquad b = 2.58, \qquad c = -1.20\,. \tag{A6}$$

This simple cubic fit reproduces the numerical results with an absolute error bounded by $0.035\beta_0^\star \approx 0.19$ (a relative error of a few percent – see Figure A5). A better fit could be obtained by using polynomials of higher order, but this level of accuracy should be adequate for most applications. With this fitting polynomial, the sphere of influence for existing structures, $r_G = (2GM_{\rm obj}/\beta^\star H_0^2)^{1/3}$, can be written in the form

$$r_G \approx 0.7\,{\rm Mpc}\left(\frac{M_{\rm obj}}{10^{12}M_\odot}\right)^{1/3} h_{70}^{-2/3}\left[1 + a(1+w) + b(1+w)^2 + c(1+w)^3\right]^{-1/3}. \tag{A7}$$

For accelerating universes, we can find the maximum distance that a light signal can propagate between now (the present epoch) and temporal infinity. This maximum distance $r_{\rm max}$ is given by

$$r_{\rm max} \equiv \int_{t_0}^{\infty}\frac{cdt}{a(t)} = \frac{c}{H_0}\int_1^\infty \frac{da}{a^2}\left[\Omega_{\rm m,0}a^{-3} + \Omega_{\rm v,0}a^{-p}\right]^{-1/2}. \tag{A8}$$

By solving the integral numerically and fitting the result, we can write the distance scale in the form

$$r_{\rm max}H_0/c \equiv I(w) \approx I_0\left[1 + \tilde{a}(1+w) + \tilde{b}(1+w)^2 + \tilde{c}(1+w)^3\right], \tag{A9}$$

where $I_0 = 1.141$, $\tilde{a} = 3.073$, $\tilde{b} = -12.39$, and $\tilde{c} = 37.13$. This fitting function is valid for the range of equations of state $-1 \le w \le -1/2$. As $w \to -1/3$, the integral (and hence $r_{\rm max}$) becomes divergent. The result is shown in Figure A6.

With the sphere of gravitational influence defined by equation (A7) and the maximum distance defined by equation (A9), we can define the isolation time $t_{\rm iso}$ for structures through the relation $a(t)r_G \ge r_{\rm max}$. The asymptotic form for the scale factor $a(t)$ is given by

$$a(t) \approx \left(\frac{p}{2}\sqrt{\Omega_{\rm v,0}}\,H_0\,t\right)^{2/p}, \tag{A10}$$

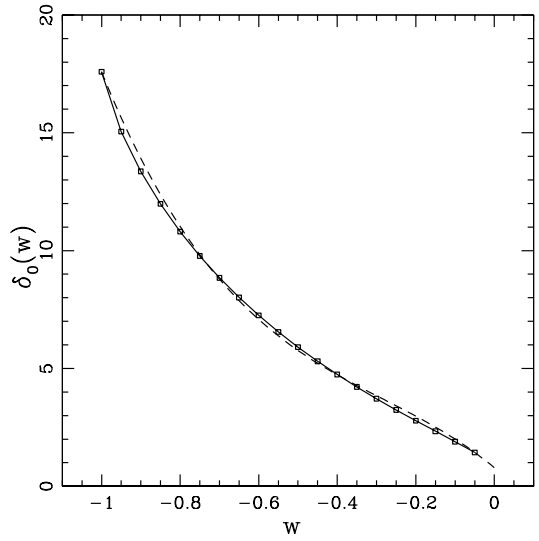

FIG. A5.— This plot shows the overdensity required for the collapse of future structures as a function of the parameter w appearing in the equation of state for quintessence models. The sphere of gravitational influence for existing cosmological structures is given by $r_G = (2GM_{\rm obj}/\beta^\star H_0^2)^{1/3}$, where the parameter $\beta^\star$ is related to the overdensity required for collapse of existing regions via $\beta^\star = \delta_0 \Omega_{\rm m,0}$ (see text). The solid curve shows the numerically determined values; the dashed curve shows a cubic fit to the function (using eqs. [A5 – A7]). As w becomes more negative, the overdensity required for collapse becomes larger and the sphere of gravitational influence (for existing structures) grows smaller — the formation of future structure is more suppressed for smaller w.

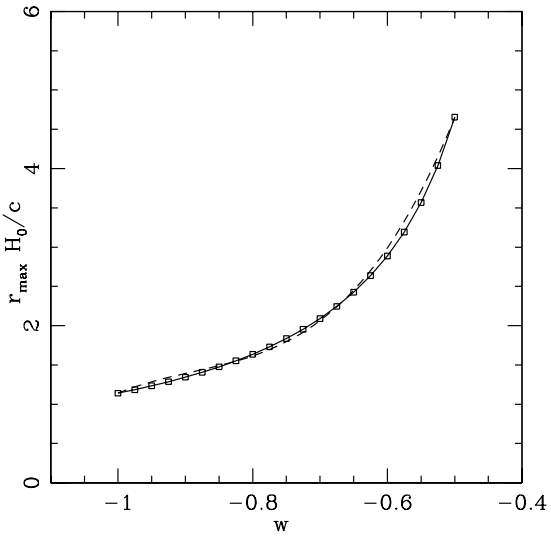

FIG. A6.— The maximum distance that a light signal can propagate between the present epoch and temporal infinity for an accelerating universe described by equation of state parameter w. The dashed curve shows a cubic fit to the numerically obtained result (see Appendix A and eq. [A9]).

where $p = 3(1+w)$ as before. The isolation time is then given by

$$t_{\rm iso} \approx \frac{2H_0^{-1}}{p\sqrt{\Omega_{\rm v,0}}} \Big\{ I(w) [\beta^\star(w)]^{1/3}\, c \left[2GM_{\rm obj}H_0\right]^{-1/3} \Big\}^{p/2} . \tag{A11}$$

Notice that this form applies only for values of p strictly greater than zero ($w > -1$). To properly take the limit $w \to -1$, $p \to 0$, the function must include additional terms that are neglected in this approximation.

B. DIMENSIONAL ANALYSIS

In this Appendix, we present a dimensional analysis that illustrates the fundamental results of this paper in simpler terms. With the benefit of hindsight, we can conceptually reproduce many of the results of this paper.

Because the universe is already dominated by its dark vacuum contribution, the future behavior of the universe is essentially one of exponential expansion at a well defined rate. This rate is set by the Hubble constant. For the sake of definiteness, we will use the asymptotic value of the Hubble constant $H_\infty = H_0\sqrt{\Omega_{\rm v,0}} \approx 59$ km s^{-1} Mpc^{-1}. This rate also defines the basic time scale for the problem, i.e., $\tau = H_\infty^{-1} = 17$ Gyr.

Using square brackets to denote the units of a given quantity (in terms of length L, time T, and mass M), we can list the variables that describe the the asymptotic universe via

$$[H_\infty] = T^{-1} \qquad [G] = L^3/MT^2 \qquad [c] = L/T\,. \tag{B1}$$

These variables can be combined to produce a dimensionless field Π_0 if only if a mass scale M_0 is introduced. The field Π_0 is then given by

$$\Pi_0 \equiv \frac{GM_0H_\infty}{c^3}\,. \tag{B2}$$

If no additional variables are introduced into the problem – no additional entities are introduced into the universe – then typically $\Pi_0 \approx 1$, which in turn defines a mass scale for the universe. Inserting numerical values, we find $M_0 \sim 10^{23} M_\odot$ (essentially the same result as that of equation [23]).

Both our physical intuition and the results of our numerical simulations indicate that cosmic structure becomes frozen and bound astronomical objects – galaxies and clusters – grow isolated in the long term. The presence of a cluster or

galaxy introduces another variable into the problem, namely the mass scale $M_{\rm obj}$. This scale, in turn, defines another dimensionless field Π_1 given by

$$\Pi_1 \equiv \frac{GM_{\rm obj}H_\infty}{c^3} \sim 10^{-11}\,, \tag{B3}$$

an incredibly small number. This quantity represents the overdensity of an isolated cluster embedded in an island universe at late times.

Next, we want to define a length scale r_0 associated with the galaxy or cluster itself. Such a length scale can be defined in several ways. The natural length scale of the universe is given by $c/H_\infty = r_H$. Since the ratio r_0/r_H is dimensionless, we expect that

$$r_0 = r_H\Pi_1^n = \frac{c}{H_\infty}\Big(\frac{GM_{\rm obj}H_\infty}{c^3}\Big)^n\,, \tag{B4}$$

where the power-law index n is to be determined. If we argue that the length scale associated with the galaxy or cluster should be non-relativistic, then n must be chosen so that the scale r_0 does not depend on the speed of light. This constraint specifies $n = 1/3$ and hence

$$r_0 = (GM_{\rm obj}/H_0^2)^{1/3}\,, \tag{B5}$$

which is the same as the gravitational sphere of influence defined by equation (11) (up to dimensionless factors of order unity). Equation (B4) allows for a second "natural" length scale – that determined by eliminating the Hubble parameter by using $n = 1$. This choice results in the scale $r = GM_{\rm obj}/c^2$, which is the length scale that determines the form of the functions $A(r)$ and $B(r)$ appearing in the metric (eq. [24]).

Another result of this investigation is the time scales for which objects become isolated and radiation is stretched "beyond the horizon". At this level of analysis, *all* of these time scales are the same and are determined by the asymptotic e-folding time $t = H_\infty^{-1} \approx 17$ Gyr. The more detailed mathematical analysis of the paper includes logarithmic correction factors, as listed in Table 1. For cosmological events, however, even the longest time scale is only 1260 Gyr or 74 e-folding times (it also turns out that $\ln[r_H/\lambda] \sim 75$ – for 'typical' astrophysical photons of wavelength $\lambda \sim 1\mu$m). For a universe with a cosmological constant, the basic result is that all future cosmological events must unfold with "nearly" the same time scale, given by H_∞^{-1}. For comparison, stellar evolution time scales are determined by more complicated physics and span a wider range of time scales, both much shorter ($\sim 10^5$ yr for star formation events; Adams & Fatuzzo 1996) and much longer ($\sim 10^{13} - 10^{14}$ yr for the duration of the longest-lived stars; AL97, LBA97). Galactic evolution – dynamical relaxation and evaporation – takes place over still longer times ($\sim 10^{20}$ yr; Dyson 1979, Binney & Tremaine 1987, AL97).

REFERENCES

Adams, F. C., & Fatuzzo, M. 1996, ApJ, 464, 256
Adams, F. C., & Laughlin, G. 1997, Rev. Mod. Phys., 69, 337
Adams, F. C., Busha, M. T., Evrard, A. E., Wechsler, R. H.. 2003, submitted to the Gravity Research Foundation's Essays on Gravitation
Balbi, A. et al. 2001, ApJ, 547, 89
Bardeen, J. 1981, Phys. Rev. Lett., 46, 382
Bennett, C. L., et al. 2003, ApJ, submitted (astro-ph/0302207)
Bialek, J.J., Evrard, A. E., & Mohr, J. J.. 2001, ApJ, 555, 597
Binney, J., & Tremaine, S. 1987, Galactic Dynamics (Princeton: Princeton Univ. Press)
Birrell, N. D., & Davies, P.C.W. 1982, Quantum Fields in Curved Space (Cambridge: Cambridge Univ. Press)
Carroll, S. M., Press, W. H., & Turner, E. L. 1992, ARA&A, 30, 499
Chieuh, T., & He, X.-G., 2002, Phys. Rev. D 65, 123518
Cirkovic, M. M. 2003, Am. J. Phys. Resource Letters, 71, 122
Cirkovic, M. M., & Samurovic, S. 2001, A & A, 373, 377
Dyson, F. J. 1979, Rev. Mod. Phys., 51, 447
Ellis, G.F.R., & Rothman, T. 1993, Am. J. Phys., 61, 883
Freedman, W. L., et al. 2001, ApJ, 553, 47
Fulling, S. A. 1977, J. Phys. A, 10, 917
Garnavich, P. H., et al. 1998, ApJ, 507, 74
Gudmundsson, E. H., & Björnsson, G. 2002, ApJ, 565, 1
Hanany, S., et al. 2000, ApJ, 545, L5
Islam, J. N. 1977, QJRAS, 18, 3
Jacoby, G. H., et al. 1992, PASP, 104, 599
Kolb, E. W., & Turner, M. S. 1990, The Early Universe (Redwood City: Addison Wesley)
Krauss, L. M., & Starkman, G. D. 2000, ApJ, 531, 22
Laughlin, G., Bodenheimer, P., & Adams, F. C. 1997, ApJ, 482, 420 (LBA97)
Limin, W., Caldwell, R. R., Ostriker, J. P, & Steinhardt, P. J. 2000, ApJ, 530, 17
Loeb, A. 2002, Phys. Rev. D 65, 047301
Lokas, E. L., & Hoffman, Y. 2001, astro-ph/0108283
Mallett, R. 1985, Phys. Rev. D 31, 416
Misner, C. W., Thorne, K. S., & Wheeler, J. A. 1973, Gravitation (San Francisco: W. H. Freeman)
Nagamine, K., & Loeb, A. 2003, NewA, 8, 439, astro-ph/0204249
Navarro, J. F., Frenk, C. S., & White S.D.M. 1997, ApJ, 490, 493 (NFW)
Peacock, J. A. 2001, Nature, 410, 169
Perlmutter, S., et al. 1998, ApJ, 517, 565
Riess, A. G., et al. 1998, AJ, 116, 1009
Springel, V., Yoshida, N., & White, S. D. M. 2001, New Astronomy, 6, 79
Spergel, D. N., et al. 2003, ApJ, submitted (astro-ph/0302209)
Starobinsky, A. A. 2000, Grav. Cosmol., 6, 157
van den Bergh, S. 1999, A & A Rev., 9, 273
Weinberg, S. 1989, Rev. Mod. Phys., 61, 1